

# Probing Higgs-Portal Dark Matter with Vector-Boson Fusion

Jan Heisig, Michael Krämer, E.M., Alexander Mück  
JHEP **03** (2020), 183

Eric Madge

Weizmann Institute of Science

PANIC – September 5, 2021

# Introduction

---

- search for Higgs portal DM in VBF
  - ▶  $m_{\text{DM}} < m_h/2$  → invisible Higgs decays, e.g. CMS – 1809.05937,  
ATLAS – 1809.06682
  - ▶  $m_{\text{DM}} > m_h/2$  → via off-shell Higgs, e.g. Ruhrdorfer et al. – 1910.04170

# Introduction

- search for Higgs portal DM in VBF
  - ▶  $m_{\text{DM}} < m_h/2 \rightarrow$  invisible Higgs decays, e.g. CMS – 1809.05937,  
ATLAS – 1809.06682
  - ▶  $m_{\text{DM}} > m_h/2 \rightarrow$  via off-shell Higgs, e.g. Ruhrdorfer et al. – 1910.04170
- here: also consider resonance region  $m_{\text{DM}} \simeq m_h/2$ 
  - motivation: can satisfy relic density and direct detection constraints
  - ⇒ need to include running width in Higgs propagator

# Introduction

- search for Higgs portal DM in VBF
  - ▶  $m_{\text{DM}} < m_h/2 \rightarrow$  invisible Higgs decays, e.g. CMS – 1809.05937,  
ATLAS – 1809.06682
  - ▶  $m_{\text{DM}} > m_h/2 \rightarrow$  via off-shell Higgs, e.g. Ruhrdorfer et al. – 1910.04170
- here: also consider resonance region  $m_{\text{DM}} \simeq m_h/2$ 
  - motivation: can satisfy relic density and direct detection constraints
  - ⇒ need to include running width in Higgs propagator
- Outline:
  - ▶ current LHC constraints: 13 TeV,  $35.9 \text{ fb}^{-1} \rightarrow$  reinterpretation of CMS search
  - ▶ limits for HL- (14 TeV,  $3 \text{ ab}^{-1}$ ) and HE-LHC (27 TeV,  $15 \text{ ab}^{-1}$ ),  
including systematics  $\rightarrow$  MC based on CMS projections

# Scalar Singlet Higgs Portal Dark Matter

- SM + real singlet scalar  $S + Z_2 \implies$  simple DM model

$$\mathcal{L} = \mathcal{L}_{\text{SM}} + \frac{1}{2}\partial_\mu S \partial^\mu S - \frac{1}{2}m_{S,0}^2 S^2 - \frac{1}{2}\lambda_S S^4 - \frac{1}{2}\lambda_{\text{HP}} S^2 \Phi^\dagger \Phi$$

- If  $m_S < \frac{m_h}{2}$ : invisible Higgs decays

$$\Gamma_{\text{inv}} = \frac{\lambda_{\text{HP}}^2 v^2}{32\pi m_h} \sqrt{1 - 4\frac{m_S^2}{m_h^2}}$$

# Scalar Singlet Higgs Portal Dark Matter

- SM + real singlet scalar  $S + Z_2 \implies$  simple DM model

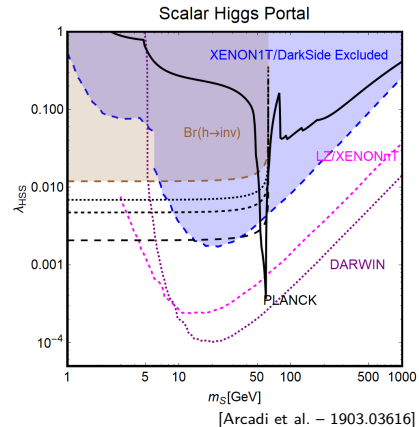
$$\mathcal{L} = \mathcal{L}_{\text{SM}} + \frac{1}{2}\partial_\mu S \partial^\mu S - \frac{1}{2}m_{S,0}^2 S^2 - \frac{1}{2}\lambda_S S^4 - \frac{1}{2}\lambda_{\text{HP}} S^2 \Phi^\dagger \Phi$$

- If  $m_S < \frac{m_h}{2}$ : invisible Higgs decays

$$\Gamma_{\text{inv}} = \frac{\lambda_{\text{HP}}^2 v^2}{32\pi m_h} \sqrt{1 - 4\frac{m_S^2}{m_h^2}}$$

- mass range favored by global fits / motivated by relic density and DM direct detection constraints:

► high masses:  $m_S \gtrsim 1 \text{ TeV}$   $\longrightarrow$  too heavy for DD



# Scalar Singlet Higgs Portal Dark Matter

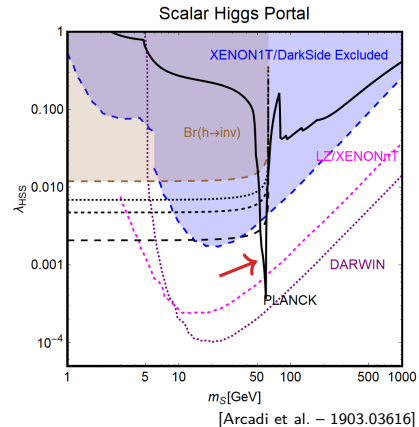
- SM + real singlet scalar  $S + Z_2 \implies$  simple DM model

$$\mathcal{L} = \mathcal{L}_{\text{SM}} + \frac{1}{2}\partial_\mu S \partial^\mu S - \frac{1}{2}m_{S,0}^2 S^2 - \frac{1}{2}\lambda_S S^4 - \frac{1}{2}\lambda_{\text{HP}} S^2 \Phi^\dagger \Phi$$

- If  $m_S < \frac{m_h}{2}$ : invisible Higgs decays

$$\Gamma_{\text{inv}} = \frac{\lambda_{\text{HP}}^2 v^2}{32\pi m_h} \sqrt{1 - 4\frac{m_S^2}{m_h^2}}$$

- mass range favored by global fits / motivated by relic density and DM direct detection constraints:
  - high masses:  $m_S \gtrsim 1 \text{ TeV}$   $\rightarrow$  too heavy for DD
  - close to  $h$  resonance:  $m_S \simeq \frac{m_h}{2}$   $\rightarrow$  small  $\lambda_{\text{HP}}$



# LHC Limits at 13 TeV

- based on CMS – 1809.05937
- search for invisible  $h$  decays in VBF:  $pp \rightarrow h + jj$ ,  $h \rightarrow \text{inv}$
- $\sqrt{s} = 13 \text{ TeV}$ ,  $\mathcal{L} = 35.9 \text{ fb}^{-1}$

# LHC Limits at 13 TeV

- based on CMS – 1809.05937
- search for invisible  $h$  decays in VBF:  $pp \rightarrow h + jj$ ,  $h \rightarrow \text{inv}$
- $\sqrt{s} = 13 \text{ TeV}$ ,  $\mathcal{L} = 35.9 \text{ fb}^{-1}$
- cuts:
$$\begin{aligned} p_T^{j_1} &> 80 \text{ GeV}, & p_T^{j_2} &> 40 \text{ GeV}, & |\eta_j| &< 4.7, \\ \eta_{j_1} \cdot \eta_{j_2} &< 0, & |\Delta\eta_{jj}| &> 4.0, & |\Delta\phi_{jj}| &< 1.5, \\ M_{jj} &> 1.3 \text{ TeV}, & \cancel{E}_T &> 250 \text{ GeV}, & \dots \end{aligned}$$

# LHC Limits at 13 TeV

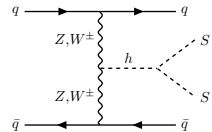
- based on CMS – 1809.05937
- search for invisible  $h$  decays in VBF:  $pp \rightarrow h + jj$ ,  $h \rightarrow \text{inv}$
- $\sqrt{s} = 13 \text{ TeV}$ ,  $\mathcal{L} = 35.9 \text{ fb}^{-1}$
- cuts:
$$p_T^{j_1} > 80 \text{ GeV}, \quad p_T^{j_2} > 40 \text{ GeV}, \quad |\eta_j| < 4.7,$$
$$\eta_{j_1} \cdot \eta_{j_2} < 0, \quad |\Delta\eta_{jj}| > 4.0, \quad |\Delta\phi_{jj}| < 1.5,$$
$$M_{jj} > 1.3 \text{ TeV}, \quad \cancel{E}_T > 250 \text{ GeV}, \quad \dots$$
- shape analysis:  $M_{jj} > 200 \text{ GeV}, \quad |\Delta\eta_{jj}| > 1.0$

# LHC Limits at 13 TeV

- based on CMS – 1809.05937
- search for invisible  $h$  decays in VBF:  $pp \rightarrow h + jj$ ,  $h \rightarrow \text{inv}$
- $\sqrt{s} = 13 \text{ TeV}$ ,  $\mathcal{L} = 35.9 \text{ fb}^{-1}$
- cuts:
$$\begin{aligned} p_T^{j_1} &> 80 \text{ GeV}, & p_T^{j_2} &> 40 \text{ GeV}, & |\eta_j| &< 4.7, \\ \eta_{j_1} \cdot \eta_{j_2} &< 0, & |\Delta\eta_{jj}| &> 4.0, & |\Delta\phi_{jj}| &< 1.5, \\ M_{jj} &> 1.3 \text{ TeV}, & \cancel{E}_T &> 250 \text{ GeV}, & \dots \end{aligned}$$
- shape analysis:  $M_{jj} > 200 \text{ GeV}$ ,  $|\Delta\eta_{jj}| > 1.0$
- 95 % CL limits on  $\mathcal{B}(h \rightarrow \text{inv})$ :
$$\mathcal{B}_{\text{inv}} < 58 \% \quad (\text{cut-and-count}) \qquad \qquad \mathcal{B}_{\text{inv}} < 33 \% \quad (\text{shape})$$

# Reinterpretation

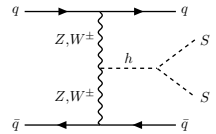
$$\sigma_{\text{inv}} = \int \frac{dq^2}{2\pi} \sigma_h(q^2) |P(q^2)|^2 2q \Gamma_{\text{inv}}(q^2) \Theta(q^2 - 4m_S^2)$$



# Reinterpretation

$$\sigma_{\text{inv}} = \int \frac{dq^2}{2\pi} \sigma_h(q^2) |P(q^2)|^2 2q \Gamma_{\text{inv}}(q^2) \Theta(q^2 - 4m_S^2)$$

off-shell Higgs  
invariant mass

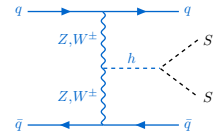


# Reinterpretation

$$\sigma_{\text{inv}} = \int \frac{dq^2}{2\pi} \sigma_h(q^2) |P(q^2)|^2 2q \Gamma_{\text{inv}}(q^2) \Theta(q^2 - 4m_S^2)$$

off-shell production cross-section

off-shell Higgs invariant mass



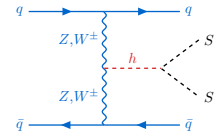
# Reinterpretation

$$\sigma_{\text{inv}} = \int \frac{dq^2}{2\pi} \sigma_h(q^2) |P(q^2)|^2 2q \Gamma_{\text{inv}}(q^2) \Theta(q^2 - 4m_S^2)$$

off-shell production cross-section

off-shell Higgs invariant mass

Higgs boson propagator



# Reinterpretation

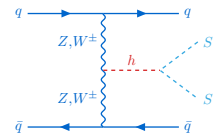
$$\sigma_{\text{inv}} = \int \frac{dq^2}{2\pi} \sigma_h(q^2) |P(q^2)|^2 2q \Gamma_{\text{inv}}(q^2) \Theta(q^2 - 4m_S^2)$$

off-shell production cross-section

off-shell Higgs invariant mass

Higgs boson propagator

invisible decay of off-shell Higgs



# Reinterpretation

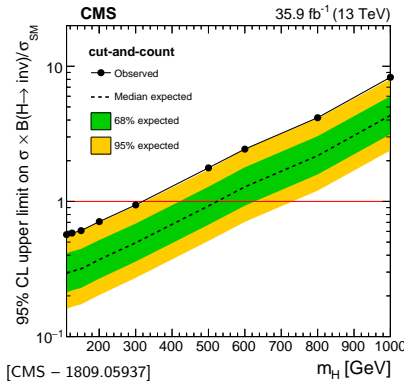
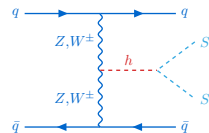
$$\sigma_{\text{inv}} = \int \frac{dq^2}{2\pi} \sigma_h(q^2) |P(q^2)|^2 2q \Gamma_{\text{inv}}(q^2) \Theta(q^2 - 4m_S^2)$$

off-shell Higgs invariant mass  
 off-shell production cross-section  
 Higgs boson propagator

- use limits on  $\mu_{\mathcal{H}} = \sigma \times \mathcal{B}(\mathcal{H} \rightarrow \text{inv}) / \sigma_{\text{SM}}$  for additional Higgs boson with mass  $m_{\mathcal{H}}$

- cut-and-count:  $\mu_{\mathcal{H}}^{95\%}(m_{\mathcal{H}}) = \frac{\sigma_{\text{inv}}^{95\%}}{\sigma_h(q^2 = m_{\mathcal{H}}^2)}$

$$\int \frac{dq^2}{2\pi} \frac{1}{\mu_{\mathcal{H}}^{95\%}(q^2)} |P(q^2)|^2 2q \Gamma_{\text{inv}}(q^2) > 1$$



# Reinterpretation

$$\sigma_{\text{inv}} = \int \frac{dq^2}{2\pi} \sigma_h(q^2) |P(q^2)|^2 2q \Gamma_{\text{inv}}(q^2) \Theta(q^2 - 4m_S^2)$$

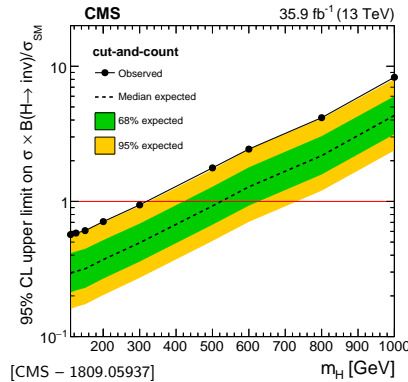
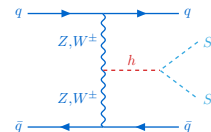
off-shell Higgs invariant mass  
 off-shell production cross-section  
 Higgs boson propagator

- use limits on  $\mu_{\mathcal{H}} = \sigma \times \mathcal{B}(\mathcal{H} \rightarrow \text{inv}) / \sigma_{\text{SM}}$  for additional Higgs boson with mass  $m_{\mathcal{H}}$

- cut-and-count:  $\mu_{\mathcal{H}}^{95\%}(m_{\mathcal{H}}) = \frac{\sigma_{\text{inv}}^{95\%}}{\sigma_h(q^2 = m_{\mathcal{H}}^2)}$

$$\int \frac{dq^2}{2\pi} \frac{1}{\mu_{\mathcal{H}}^{95\%}(q^2)} |P(q^2)|^2 2q \Gamma_{\text{inv}}(q^2) > 1$$

- same procedure for shape analysis:  
assumption:  $M_{jj}$  and  $|\Delta\eta_{jj}|$  distributions only weakly  $q^2$  dependent



# Higgs Propagator

Resummed propagator:

$$|P(q^2)|^2 = \left| \frac{i}{q^2 - m_R^2 + \Sigma(q^2) + i\varepsilon} \right|^2$$

# Higgs Propagator

Resummed propagator:

$$\left| P(q^2) \right|^2 = \left| \frac{i}{q^2 - m_R^2 + \Sigma(q^2) + i\varepsilon} \right|^2 \stackrel{\text{close to the resonance:}}{\simeq} \left| \frac{i}{q^2 - m_P^2 + i m_P \Gamma_{\text{tot}}} \right|^2$$

close to the resonance:  
Breit-Wigner propagator

# Higgs Propagator

Resummed propagator:

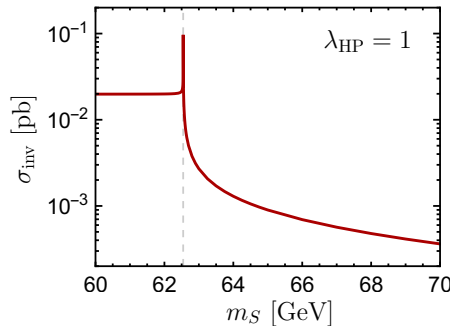
$$\left| P(q^2) \right|^2 = \left| \frac{i}{q^2 - m_R^2 + \Sigma(q^2) + i\varepsilon} \right|^2 \stackrel{\text{close to the resonance:}}{\simeq} \left| \frac{i}{q^2 - m_P^2 + i m_P \Gamma_{\text{tot}}} \right|^2 \stackrel{\text{NWA: } \Gamma_{\text{tot}} \ll m_P}{\simeq} \frac{\pi}{m_P \Gamma_{\text{tot}}} \delta(q^2 - m_P^2)$$

# Higgs Propagator

Resummed propagator:

$$\left|P(q^2)\right|^2 = \left| \frac{i}{q^2 - m_R^2 + \Sigma(q^2) + i\varepsilon} \right|^2 \stackrel{\text{close to the resonance:}}{\underset{\text{Breit-Wigner propagator}}{\approx}} \left| \frac{i}{q^2 - m_P^2 + i m_P \Gamma_{\text{tot}}} \right|^2 \stackrel{\text{NWA: } \Gamma_{\text{tot}} \ll m_P}{\approx} \frac{\pi}{m_P \Gamma_{\text{tot}}} \delta(q^2 - m_P^2)$$

- fixed-width prescription only works if  $\Gamma_{\text{tot}} \sim \text{const}$  in the resonance region  
→ fails if large decay channel opens close to resonance, i.e. for  $m_S \gtrsim \frac{m_h}{2}$ ,  $\lambda_{\text{HP}} \gtrsim 0.1$



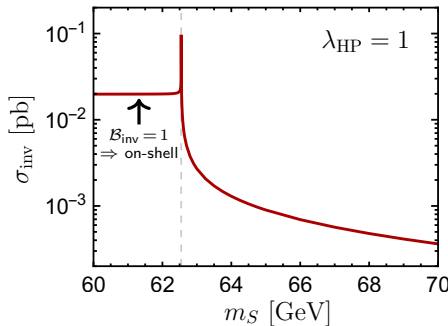
# Higgs Propagator

Resummed propagator:

$$\left|P(q^2)\right|^2 = \left| \frac{i}{q^2 - m_R^2 + \Sigma(q^2) + i\varepsilon} \right|^2 \stackrel{\text{close to the resonance:}}{\simeq} \left| \frac{i}{q^2 - m_P^2 + i m_P \Gamma_{\text{tot}}} \right|^2 \stackrel{\text{NWA: } \Gamma_{\text{tot}} \ll m_P}{\simeq} \frac{\pi}{m_P \Gamma_{\text{tot}}} \delta(q^2 - m_P^2)$$

close to the resonance:  
Breit-Wigner propagator

- fixed-width prescription only works if  $\Gamma_{\text{tot}} \sim \text{const}$  in the resonance region  
→ fails if large decay channel opens close to resonance, i.e. for  $m_S \gtrsim \frac{m_h}{2}$ ,  $\lambda_{\text{HP}} \gtrsim 0.1$



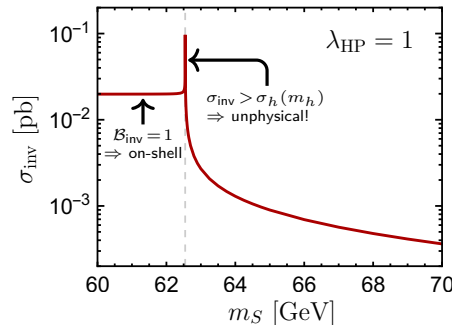
# Higgs Propagator

Resummed propagator:

$$\left|P(q^2)\right|^2 = \left| \frac{i}{q^2 - m_R^2 + \Sigma(q^2) + i\varepsilon} \right|^2 \stackrel{\text{close to the resonance:}}{\simeq} \left| \frac{i}{q^2 - m_P^2 + i m_P \Gamma_{\text{tot}}} \right|^2 \stackrel{\text{NWA: } \Gamma_{\text{tot}} \ll m_P}{\simeq} \frac{\pi}{m_P \Gamma_{\text{tot}}} \delta(q^2 - m_P^2)$$

Breit-Wigner propagator

- fixed-width prescription only works if  $\Gamma_{\text{tot}} \sim \text{const}$  in the resonance region  
fails if large decay channel opens close to resonance, i.e. for  $m_S \gtrsim \frac{m_h}{2}$ ,  $\lambda_{\text{HP}} \gtrsim 0.1$



# Higgs Propagator

Resummed propagator:

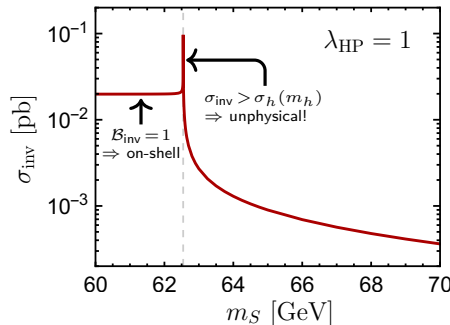
$$\left|P(q^2)\right|^2 = \left| \frac{i}{q^2 - m_R^2 + \Sigma(q^2) + i\varepsilon} \right|^2 \stackrel{\text{close to the resonance:}}{\approx} \left| \frac{i}{q^2 - m_P^2 + i m_P \Gamma_{\text{tot}}} \right|^2 \stackrel{\text{NWA: } \Gamma_{\text{tot}} \ll m_P}{\approx} \frac{\pi}{m_P \Gamma_{\text{tot}}} \delta(q^2 - m_P^2)$$

↑  
Breit-Wigner propagator

- fixed-width prescription only works if  $\Gamma_{\text{tot}} \sim \text{const}$  in the resonance region  
→ fails if large decay channel opens close to resonance, i.e. for  $m_S \gtrsim \frac{m_h}{2}$ ,  $\lambda_{\text{HP}} \gtrsim 0.1$
- use running-width propagator:

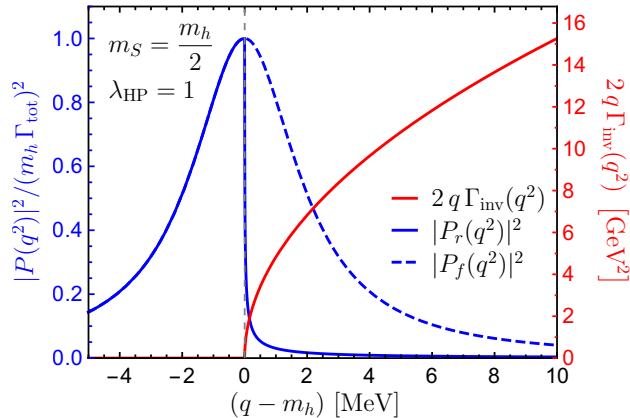
$$P_r(q^2) = \frac{i}{q^2 - m_h^2 + i \sqrt{q^2} \Gamma_{\text{tot}}(q^2)}$$

here:  $\Gamma_{\text{tot}}(q^2) = \Gamma_h^{\text{SM}} + \Gamma_{\text{inv}}(q^2)$



# Running Width vs. Fixed Width at $m_S \simeq m_h/2$

Problem:  $2q\Gamma_{\text{inv}}(q^2)$  grows rapidly for  $q^2$  slightly above  $(2m_S)^2$ , but fixed-width propagator does not know about the opening invisible channel



Recall:  $\sigma_{\text{inv}} = \int \frac{dq^2}{2\pi} \sigma_h(q^2) |P(q^2)|^2 2q\Gamma_{\text{inv}}(q^2)$

# Running Width vs. Fixed Width at $m_S \simeq m_h/2$

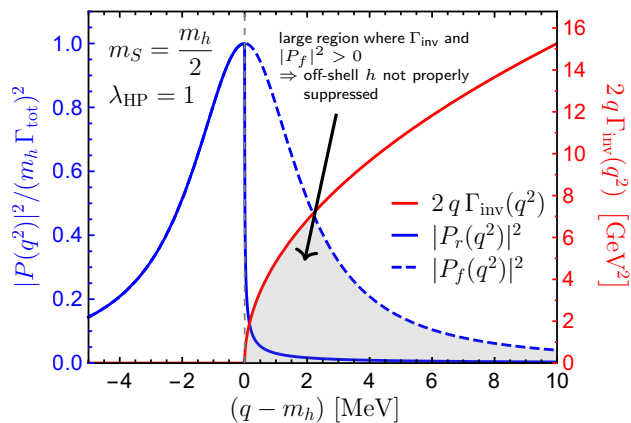
**Problem:**  $2q\Gamma_{\text{inv}}(q^2)$  grows rapidly for  $q^2$  slightly above  $(2m_S)^2$ , but fixed-width propagator does not know about the opening invisible channel

consider  $2q\Gamma_{\text{inv}}(q^2)|P(q^2)|^2$  just above resonance ( $q^2 \approx m_h^2$ ):

fixed width:

$$\frac{2q\Gamma_{\text{inv}}(q^2)}{m_h^2\Gamma_{\text{tot}}^2(m_h^2)} \gg 1$$

Recall:  $\sigma_{\text{inv}} = \int \frac{dq^2}{2\pi} \sigma_h(q^2) |P(q^2)|^2 2q\Gamma_{\text{inv}}(q^2)$



# Running Width vs. Fixed Width at $m_S \simeq m_h/2$

**Problem:**  $2q\Gamma_{\text{inv}}(q^2)$  grows rapidly for  $q^2$  slightly above  $(2m_S)^2$ , but fixed-width propagator does not know about the opening invisible channel

consider  $2q\Gamma_{\text{inv}}(q^2)|P(q^2)|^2$  just above resonance ( $q^2 \approx m_h^2$ ):

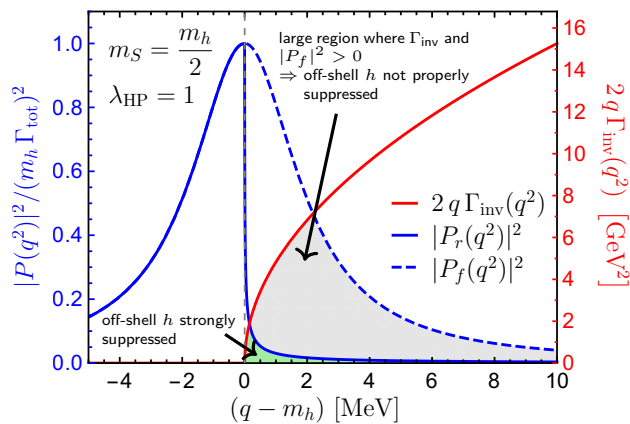
fixed width:

$$\frac{2q\Gamma_{\text{inv}}(q^2)}{m_h^2\Gamma_{\text{tot}}^2(m_h^2)} \gg 1$$

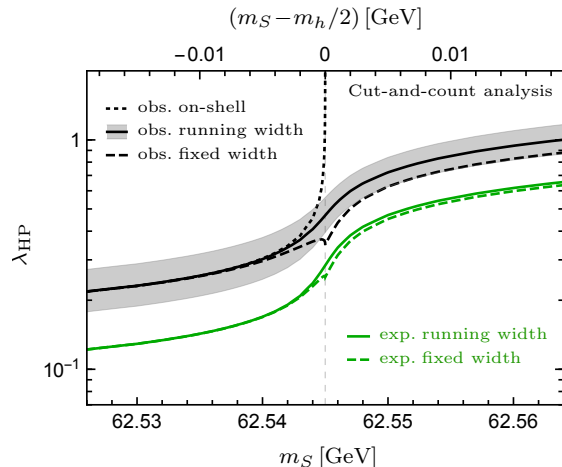
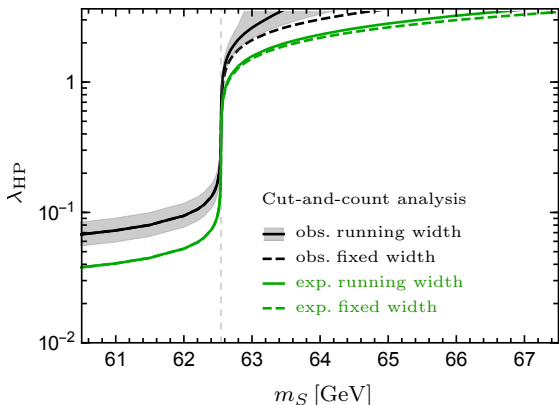
running width:

$$\frac{2q\Gamma_{\text{inv}}(q^2)}{q^2\Gamma_{\text{tot}}^2(q^2)} \sim \frac{2}{q\Gamma_{\text{inv}}(q^2)}$$

Recall:  $\sigma_{\text{inv}} = \int \frac{dq^2}{2\pi} \sigma_h(q^2) |P(q^2)|^2 2q\Gamma_{\text{inv}}(q^2)$



# 13 TeV Results – Cut and Count

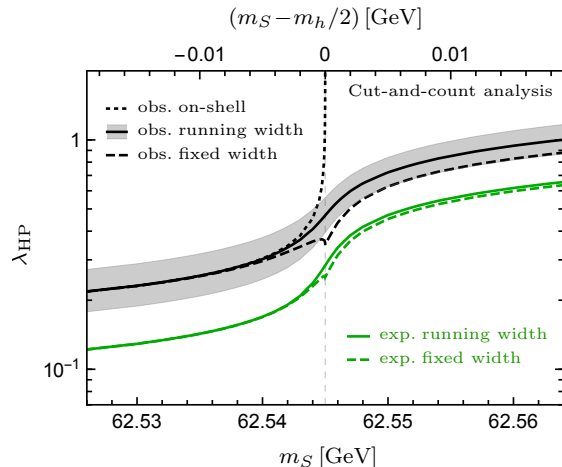
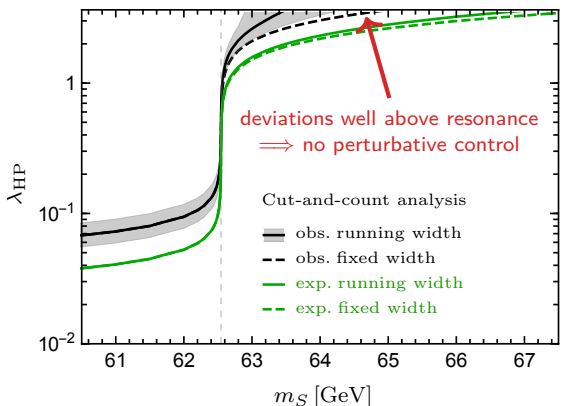


observed (expected) limits:

$\mathcal{B}(h \rightarrow \text{inv}) < 58\% \ (30\%)$

[CMS – 1809.05937]

# 13 TeV Results – Cut and Count

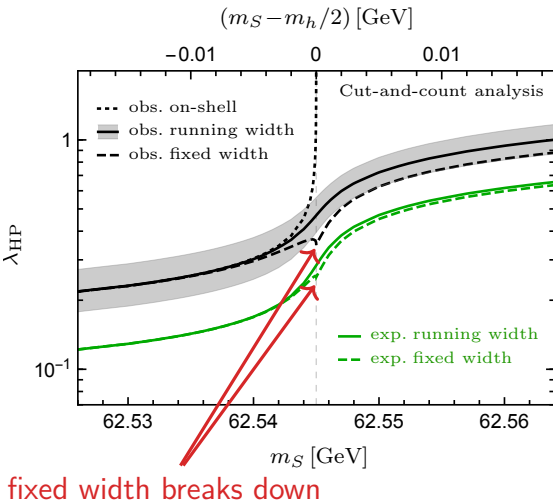
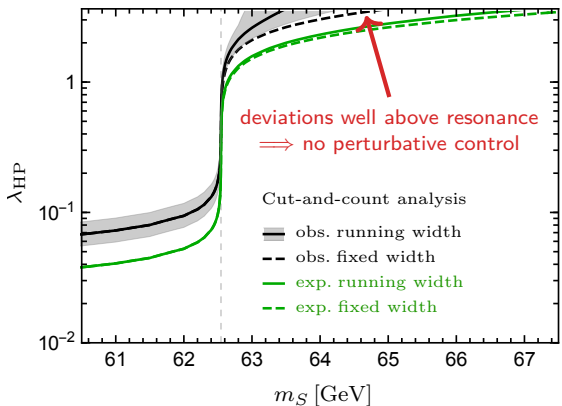


observed (expected) limits:

$\mathcal{B}(h \rightarrow \text{inv}) < 58\% \ (30\%)$

[CMS – 1809.05937]

# 13 TeV Results – Cut and Count

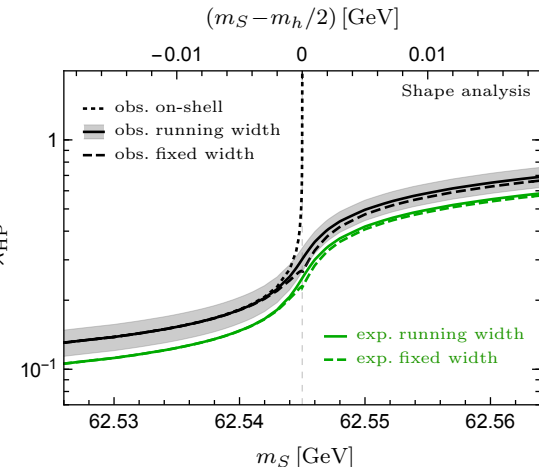
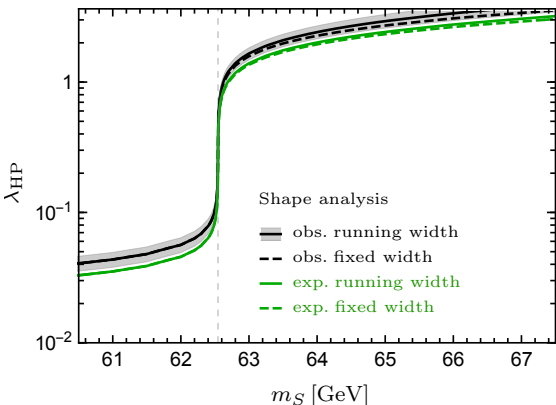


observed (expected) limits:

$$\mathcal{B}(h \rightarrow \text{inv}) < 58\% \text{ (30\%)}$$

[CMS – 1809.05937]

# 13 TeV Results – Shape Analysis

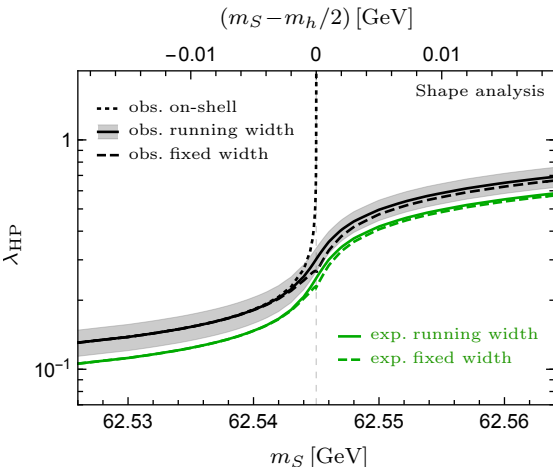
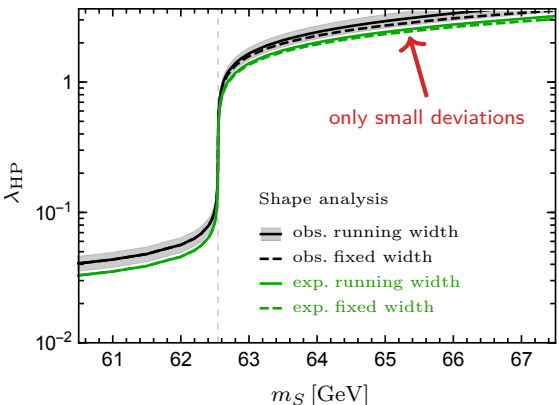


observed (expected) limits:

$\mathcal{B}(h \rightarrow \text{inv}) < 33\% \ (25\%)$

[CMS – 1809.05937]

# 13 TeV Results – Shape Analysis

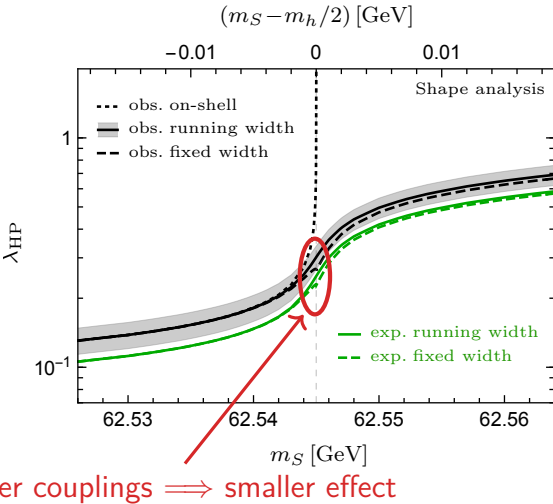
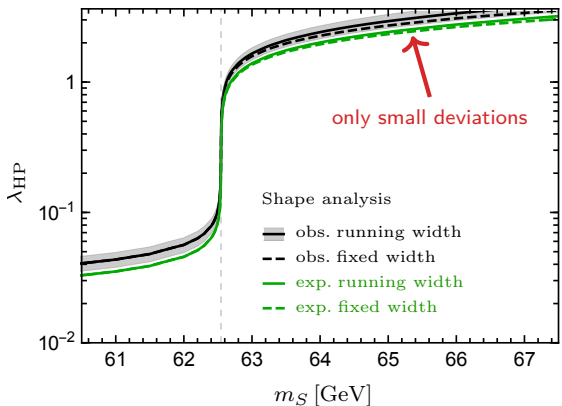


observed (expected) limits:

$\mathcal{B}(h \rightarrow \text{inv}) < 33\% \text{ (25\%)}$

[CMS – 1809.05937]

# 13 TeV Results – Shape Analysis



observed (expected) limits:

$$\mathcal{B}(h \rightarrow \text{inv}) < 33\% \text{ (25\%)}$$

[CMS – 1809.05937]

# HL- and HE-LHC Projections

- HL-LHC:  $\sqrt{s} = 14 \text{ TeV}$ ,  $\mathcal{L} = 3 \text{ ab}^{-1}$  [CMS-PAS-FTR-18-016]

14 TeV projections for invisible  $h$  in VBF by CMS:  $\mathcal{B}(h \rightarrow \text{inv}) < 3.8 \%$

- ▶ higher  $M_{jj}$  and lower  $\cancel{E}_T$  cut:  $M_{jj} > 2.5 \text{ TeV}$ ,  $\cancel{E}_T > 190 \text{ GeV}$
  - ▶ provides prediction for on-shell Higgs production and background events
  - ▶ includes systematic uncertainties
- ⇒ still needed: cross section for off-shell/additional Higgs boson

# HL- and HE-LHC Projections

- HL-LHC:  $\sqrt{s} = 14 \text{ TeV}$ ,  $\mathcal{L} = 3 \text{ ab}^{-1}$  [CMS-PAS-FTR-18-016]
  - 14 TeV projections for invisible  $h$  in VBF by CMS:  $\mathcal{B}(h \rightarrow \text{inv}) < 3.8 \%$
  - ▶ higher  $M_{jj}$  and lower  $\cancel{E}_T$  cut:  $M_{jj} > 2.5 \text{ TeV}$ ,  $\cancel{E}_T > 190 \text{ GeV}$
  - ▶ provides prediction for on-shell Higgs production and background events
  - ▶ includes systematic uncertainties
  - ⇒ still needed: cross section for off-shell/additional Higgs boson
- HE-LHC:  $\sqrt{s} = 27 \text{ TeV}$ ,  $\mathcal{L} = 15 \text{ ab}^{-1}$ 
  - ▶ generate signal (on/off-shell) and background events → MC simulation
  - ▶ determine sensitivity including systematics → extracted from HL-LHC
  - ▶ optimize  $M_{jj}$  cut →  $M_{jj} > 6 \text{ TeV}$

# Systematic Uncertainties

- 95 % CL limit:

$$\frac{S}{\sqrt{S + B + (\sigma_B^{\text{sys}} B)^2}} = 1.96$$

# Systematic Uncertainties

- 95 % CL limit:

$$\frac{S}{\sqrt{S + B + (\sigma_B^{\text{sys}} B)^2}} = 1.96$$

- model for systematic uncertainties:

$$\sigma_B^{\text{sys}} = \sqrt{\frac{f}{B} + (\sigma_B^{\text{ind}})^2}$$

↑ scales with  $1/\mathcal{L}$   
e.g. data-driven background determination

↑ luminosity independent  
e.g. transfer factors from control to signal region

# Systematic Uncertainties

- 95 % CL limit:

$$\frac{S}{\sqrt{S + B + (\sigma_B^{\text{sys}} B)^2}} = 1.96$$

- model for systematic uncertainties:

$$\sigma_B^{\text{sys}} = \sqrt{f/B + (\sigma_B^{\text{ind}})^2}$$

scales with  $1/\mathcal{L}$

e.g. data-driven background determination

luminosity independent

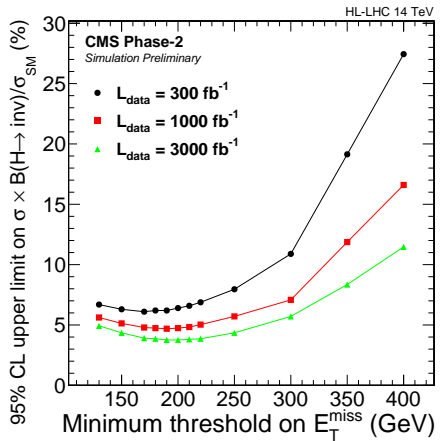
e.g. transfer factors from control to signal region

- extract parameters from limits for different  $\mathcal{L}$ :

$$f = 1.5$$

$$\sigma_B^{\text{ind}} = 1.3\%$$

- use same parameters for HE-LHC projections



[CMS-PAS-FTR-18-016]

# 14 and 27 TeV Results

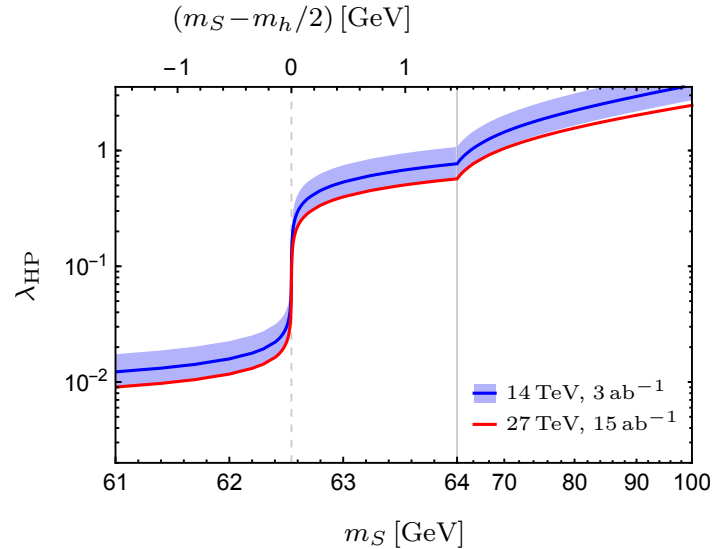
- at  $m_S = m_h/2$ :

HL-LHC:  $\lambda_{\text{HP}} < 0.090$

HE-LHC:  $\lambda_{\text{HP}} < 0.067$

➡ no visible effect of running  
vs. fixed width

- HE-LHC:  $\mathcal{B}(h \rightarrow \text{inv}) \leq 2.1\%$



# Summary

- VBF promising channel to search for Higgs portal DM
- special attention: Higgs resonance  $m_S \simeq m_h/2$ 

⇒ requires running-width propagator!

fixed-width calculation overestimates exclusion reach by 30% (15%)  
for 13 TeV cut-and-count (shape) analysis
- limits on  $\lambda_{\text{HP}}$ :  $m_S = 61 \text{ GeV} \quad m_h/2 \quad 64 \text{ GeV}$ 

LHC:	0.04	0.3	2.5
HL-LHC:	0.01	0.09	0.8
HE-LHC:	0.009	0.07	0.6
- limits on  $\mu_{\mathcal{H}}$  and  $\lambda_{\text{HP}}$  are available as supplementary material to [\[1912.08472\]](#)

# Summary

- VBF promising channel to search for Higgs portal DM
- special attention: Higgs resonance  $m_S \simeq m_h/2$   
     $\Rightarrow$  requires running-width propagator!  
        fixed-width calculation overestimates exclusion reach by 30% (15%)  
        for 13 TeV cut-and-count (shape) analysis
- limits on  $\lambda_{\text{HP}}$ :  $m_S = 61 \text{ GeV} \quad m_h/2 \quad 64 \text{ GeV}$ 

LHC:	0.04	0.3	2.5
HL-LHC:	0.01	0.09	0.8
HE-LHC:	0.009	0.07	0.6
- limits on  $\mu_{\mathcal{H}}$  and  $\lambda_{\text{HP}}$  are available as supplementary material to [\[1912.08472\]](#)

Thank you for your attention!

# Backup

# Fermion, Vector, and Tensor Dark Matter

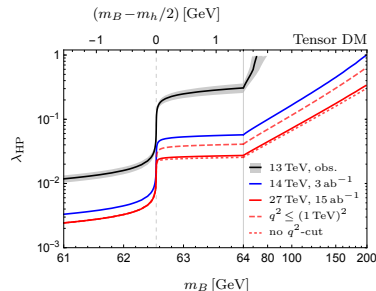
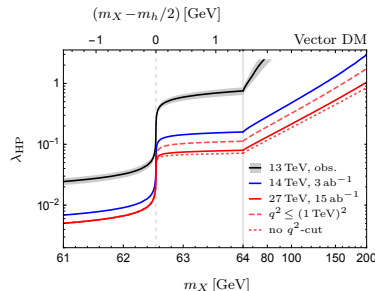
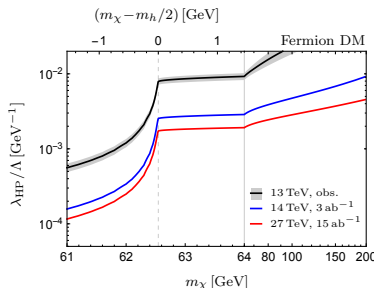
other choices for DM candidate:

- Majorana fermion  $\chi$
- vector  $X^\mu$
- anti-symmetric tensor  $B^{\mu\nu}$

$$\mathcal{L}_{\text{HP}} = -\frac{\lambda_{\text{HP}}}{\Lambda} \Phi^\dagger \Phi \bar{\chi}\chi$$
$$\mathcal{L}_{\text{HP}} = -\frac{\lambda_{\text{HP}}}{2} \Phi^\dagger \Phi X^\mu X_\mu$$
$$\mathcal{L}_{\text{HP}} = -\frac{\lambda_{\text{HP}}}{2} \Phi^\dagger \Phi B^{\mu\nu} B_{\mu\nu}$$

Kanemura et al. – 1005.5651  
Cata, Ibarra – 1404.0432  
Endo, Takaesu – 1407.6882

not UV complete!



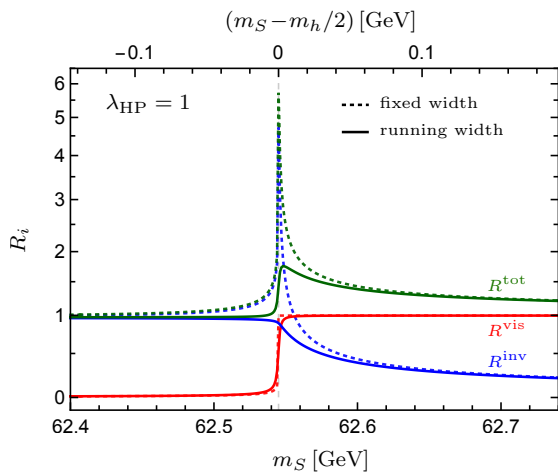
# Running Width Propagator

Consider  $R_i^X \simeq \frac{\sigma_i^X}{\sigma_h(m_h^2)}$ :

$$R_f^X = \int \frac{dq^2}{2\pi} \frac{2q \Gamma_X(q^2)}{(q^2 - m_h^2)^2 + m_h^2 \Gamma_{\text{tot}}^2(m_h^2)}$$

$$R_r^X = \int \frac{dq^2}{2\pi} \frac{2q \Gamma_X(q^2)}{(q^2 - m_h^2)^2 + q^2 \Gamma_{\text{tot}}^2(q^2)}$$

- **fixed width:** (for  $m_S \simeq m_h/2$ )  
 $\sigma_f^{\text{tot}}$  not related to  $\sigma_h(m_h^2)$  any more
- **running width:**  
smooth transition between on- and off-shell region

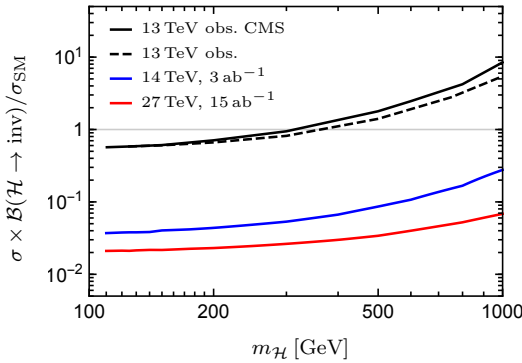


# MC Simulation

- tool chain: MadGraph5 → PYTHIA8 → Delphes
- simulate VBF  $h$  production  
 $(pp \rightarrow \mathcal{H} + 2 \text{ jets})$   
at LO for  $m_{\mathcal{H}} = 100 \text{ GeV} - 1 \text{ TeV}$
- ggF contribution:  
rescale to on-shell CMS prediction  
(also: NLO/detector effects)
  - ▶ 13 TeV :  $\sigma_h^{\text{CMS}} / \sigma_h^{\text{MC}} = 1.46$
  - ▶ 14 TeV :  $\sigma_h^{\text{CMS}} / \sigma_h^{\text{MC}} = 1.54$  ← also for HE-LHC
- background at 27 TeV:  
MC simulation of  $Z/W + 2-3 \text{ jets}$ , rescaled based on HL-LHC predictions

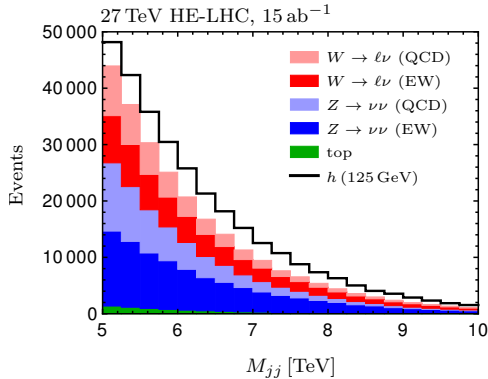
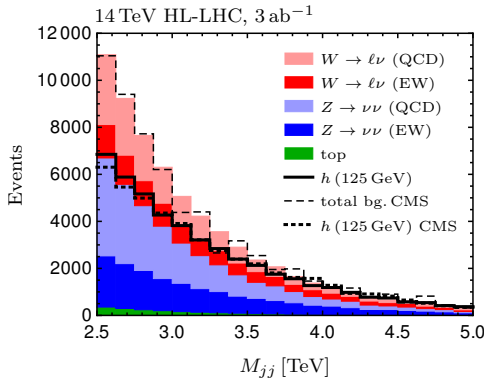
# MC Simulation

- tool chain: MadGraph5 → PYTHIA8 → Delphes
- simulate VBF  $h$  production ( $pp \rightarrow \mathcal{H} + 2$  jets) at LO for  $m_{\mathcal{H}} = 100$  GeV – 1 TeV
- ggF contribution:  
rescale to on-shell CMS prediction  
(also: NLO/detector effects)
  - ▶ 13 TeV :  $\sigma_h^{\text{CMS}} / \sigma_h^{\text{MC}} = 1.46$
  - ▶ 14 TeV :  $\sigma_h^{\text{CMS}} / \sigma_h^{\text{MC}} = 1.54$  ← also for HE-LHC
- background at 27 TeV:  
MC simulation of  $Z/W + 2-3$  jets, rescaled based on HL-LHC predictions



# 27 TeV Background Predictions

- MC simulation:  $Z/W + 2$  or  $3$  jets using MLM merging
- rescale background contributions based on 14 TeV CMS predictions
- top + jets included in  $W +$  jets rescaling



- optimized  $M_{jj}$  cut for  $m_h = 125.09 \text{ GeV}$   $\implies M_{jj} > 6 \text{ TeV}$